

## Evidence for a highly deformed band in $^{16}\text{O} + ^{16}\text{O}$ breakup of $^{32}\text{S}$

N. Curtis,<sup>\*</sup> A. St. J. Murphy, N. M. Clarke, M. Freer, B. R. Fulton, S. J. Hall, M. J. Leddy,<sup>†</sup> J. S. Pople,<sup>‡</sup> G. Tungate,  
and R. P. Ward<sup>§</sup>

*School of Physics and Space Research, University of Birmingham, Edgbaston, Birmingham B15 2TT, United Kingdom*

W. N. Catford, G. J. Gyapong, and S. M. Singer

*Department of Physics, University of Surrey, Guildford, Surrey GU2 5XH, United Kingdom*

S. P. G. Chappell, S. P. Fox, C. D. Jones, and D. L. Watson

*Department of Physics, University of York, Heslington, York YO1 5DD, United Kingdom*

W. D. M. Rae and P. M. Simmons

*Department of Nuclear Physics, University of Oxford, Keble Road, Oxford OX1 3RH, United Kingdom*

P. H. Regan<sup>||</sup>

*Department of Nuclear Physics, Research School of Physical Sciences, Australian National University,  
GPO Box 4, Canberra, ACT 2601, Australia*

(Received 2 October 1995)

A study of the  $^{12}\text{C}(^{24}\text{Mg}, ^{16}\text{O})^4\text{He}$  reaction has revealed  $^{16}\text{O} + ^{16}\text{O}$  breakup from states in  $^{32}\text{S}$  in the excitation region ranging from 32 to 38 MeV. The spins of the states near 33, 35, and 38 MeV of excitation, obtained from angular correlations, are measured to be  $(10^+ \text{ or } 12^+)$ ,  $(12^+ \text{ or } 14^+)$ , and  $(14^+ \text{ or } 16^+)$ , respectively. These may be interpreted as arising from a highly deformed band in  $^{32}\text{S}$ .

PACS number(s): 25.70.Ef, 21.10.Re, 27.30.+t

### I. INTRODUCTION

In recent years the breakup of  $^{24}\text{Mg}$  to  $^{12}\text{C} + ^{12}\text{C}$  has been observed in a number of experiments [1–6]. Breakup is seen to occur from discrete states in the excited  $^{24}\text{Mg}$  nucleus in the excitation range 20–30 MeV. This is also the excitation region in which the quasimolecular or barrier resonances have been seen in  $^{12}\text{C} + ^{12}\text{C}$  scattering measurements [7], and recently an association between these resonances and the breakup states has been proposed following a high resolution breakup measurement [8]. This has led to speculation that such a breakup may also be observed in  $^{28}\text{Si}$  and  $^{32}\text{S}$ , since resonances are also observed in  $^{12}\text{C} + ^{16}\text{O}$  and  $^{16}\text{O} + ^{16}\text{O}$  scattering studies [7].

Bennett *et al.* [9] have previously reported evidence for the breakup of  $^{28}\text{Si}$  to  $^{12}\text{C} + ^{16}\text{O}$  and  $^{32}\text{S}$  to  $^{16}\text{O} + ^{16}\text{O}$ . They found that this breakup depends on how these nuclei are excited, suggesting that the breakup states correspond to specific configurations. These observations are in agreement

with various theoretical calculations which have predicted the existence of deformed shape isomers in many light alpha conjugate nuclei, ranging from  $^{12}\text{C}$  to  $^{44}\text{Ti}$ , and including  $^{28}\text{Si}$  and  $^{32}\text{S}$ . These calculations include the Nilsson-Strutinsky calculations of Leander and Larsson [10], the Hartree-Fock calculations of Flocard *et al.* [11], and the Bloch-Brink alpha cluster model calculations of Zhang, Rae, and Merchant [12]. However, although the measurement by Bennett *et al.* showed yield in the  $^{16}\text{O} + ^{16}\text{O}$  breakup channel, they were unable to show that this corresponded to decays from specific states in the  $^{32}\text{S}$  nucleus. Hence it is important to study this breakup process in more detail than the earlier measurement allowed.

In this paper we report evidence for the breakup of  $^{32}\text{S}$  to  $^{16}\text{O} + ^{16}\text{O}$  observed in the  $^{12}\text{C}(^{24}\text{Mg}, ^{16}\text{O})^4\text{He}$  reaction. Bennett *et al.* [9] have used the Harvey rules [13] to show that the formation of a configuration in  $^{32}\text{S}$  which can decay via  $^{16}\text{O} + ^{16}\text{O}$  is precluded when using a  $^{32}\text{S}$  projectile or an  $\alpha$  pickup reaction onto a  $^{28}\text{Si}$  projectile, but is allowed with a double- $\alpha$  (or  $^8\text{Be}$ ) transfer reaction onto a  $^{24}\text{Mg}$  projectile. The Harvey rules emerge naturally from considerations of the Pauli principle and have been discussed by Mosel [14] in the context of a two-center shell model, and by Freer *et al.* [15] in the context of the two-center harmonic oscillator.

### II. EXPERIMENTAL DETAILS

The experiment was performed using a 170 MeV  $^{24}\text{Mg}$  beam, provided by the 14UD tandem accelerator of the Department of Nuclear Physics at the Australian National University. The beam was incident on a  $450 \mu\text{g cm}^{-2}$  natural carbon target. Coincident  $^{16}\text{O}$  nuclei from the breakup of the

<sup>\*</sup>Present address: Department of Physics, University of Surrey, Guildford, Surrey, GU2 5XH, United Kingdom.

<sup>†</sup>Present address: Department of Physics, University of Manchester, Manchester, M13 9PL, United Kingdom.

<sup>‡</sup>Present address: Defence Research Establishment Malvern, St. Andrews Road, Great Malvern, Worcestershire, WR14 3PS, United Kingdom.

<sup>§</sup>Present address: School of Sciences, University of Staffordshire, College Road, Stoke on Trent, ST4 2DE, United Kingdom.

<sup>||</sup>Present address: Department of Physics, University of Surrey, Guildford, Surrey, GU2 5XH, United Kingdom.

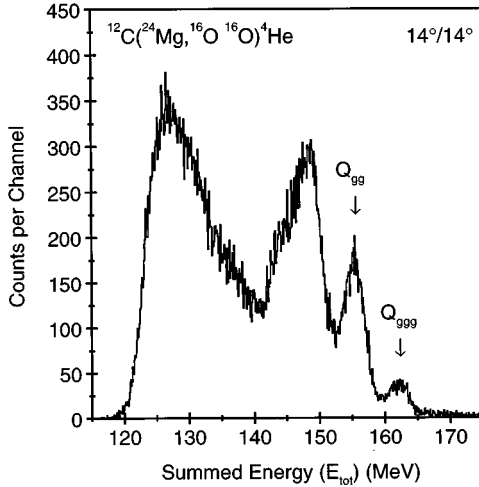


FIG. 1. Total energy spectrum for  $^{16}\text{O} + ^{16}\text{O}$  breakup of  $^{32}\text{S}$  at arm angle settings of  $14^\circ/14^\circ$ .

excited  $^{32}\text{S}$  nucleus following the  $^{12}\text{C}(^{24}\text{Mg}, ^{16}\text{O} ^{16}\text{O})^4\text{He}$  reaction were detected in two gas-silicon hybrid detector telescopes placed on either side of the beam on movable arms. Each hybrid telescope consisted of two detectors. At the front of the hybrid was a 50 mm thick gas ionization chamber filled to 120 torr with propane which acted as a  $\Delta E$  detector. At the rear of the gas region was a position sensitive silicon strip detector, comprised of 16 independent horizontal strips fabricated onto a single  $50\text{ mm} \times 50\text{ mm}$  silicon slice. The silicon detector provided both position and energy information and when used in conjunction with the gas detector also provided  $\Delta E$ - $E$  particle identification. A more detailed description of the hybrid detectors has been given by Curtis *et al.* [16]. The target to silicon detector distance for this experiment was 235 mm, and two pairs of arm angle settings were used,  $14^\circ/14^\circ$  and  $18^\circ/18^\circ$ . The angular acceptance of each detector telescope was 45 msr. The beam exposures at the two arm angle settings were 0.8 mC and 2.3 mC, respectively.

### III. RESULTS AND DISCUSSION

Figure 1 shows the total energy ( $E_{\text{tot}}$ ) spectrum obtained from the coincident detection of the two  $^{16}\text{O}$  nuclei at the  $14^\circ/14^\circ$  arm angle setting. The quantity  $E_{\text{tot}}$  is the sum of the energies of the two detected nuclei and the third undetected recoiling particle (which is determined by using momentum conservation between the two detected fragments and the beam, assuming a three-body final state). The peak labeled  $Q_{ggg}$  corresponds to events where all three exit channel particles emerge in their ground states, and thus lies at an energy equal to the sum of the beam energy and the three-body reaction  $Q$  value. For the  $^{12}\text{C}(^{24}\text{Mg}, ^{16}\text{O} ^{16}\text{O})^4\text{He}$  reaction this  $Q$  value is equal to  $-6.883\text{ MeV}$ . The measured width of the  $Q_{ggg}$  peak is  $(2800 \pm 250)\text{ keV}$ . This value agrees well with the  $(2700 \pm 400)\text{ keV}$  predicted by a Monte Carlo code that has been developed to simulate breakup reactions [8]. This simulation includes the effects of interactions of the beam and breakup fragments in the target, the detector performance, and the reaction kinematics. The Monte Carlo results show that it is the differential energy loss between the

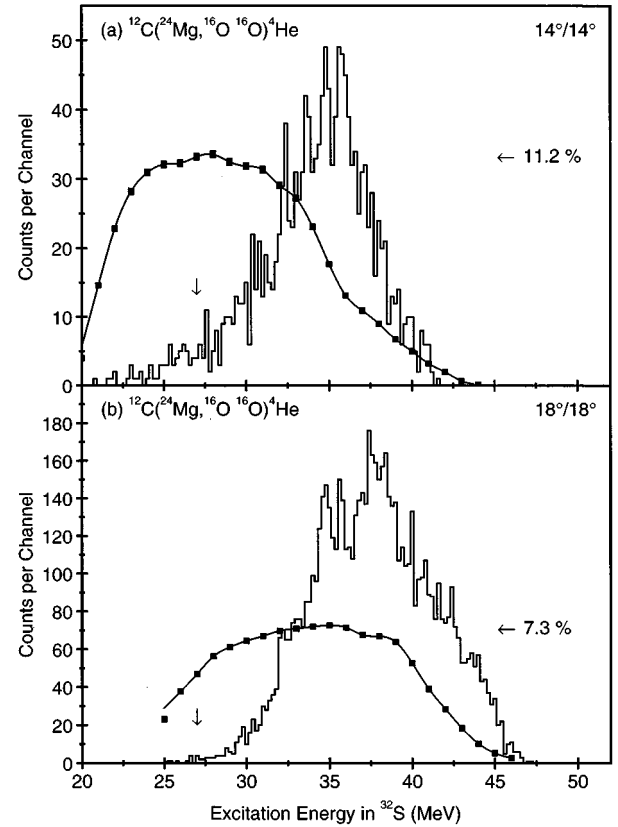


FIG. 2. Excitation energy spectrum for  $^{16}\text{O} + ^{16}\text{O}$  breakup of  $^{32}\text{S}$  at (a) arm angle settings of  $14^\circ/14^\circ$  and (b) arm angle settings of  $18^\circ/18^\circ$ . The detector efficiency profiles are shown by the solid curve through the solid squares, the peak values being indicated. The classical Coulomb barrier position is indicated by the vertical arrow.

beam and fragments in the target that dominates the  $E_{\text{tot}}$  resolution. The lower peak in Fig. 1, labeled  $Q_{gg}$ , corresponds to events in which one of the two  $^{16}\text{O}$  nuclei is emitted in either its first or second excited state (6.05 MeV, and 6.13 MeV, respectively).

By gating on events falling within the  $Q_{ggg}$  peak the excitation of the resonant  $^{32}\text{S}$  nucleus can be determined by calculating the relative energy between the two  $^{16}\text{O}$  fragments for each event. The question as to whether the two  $^{16}\text{O}$  fragments do indeed arise from a common  $^{32}\text{S}$  parent will be discussed below. The process by which the excitation energy is determined is described in more detail in Ref. [16].

Figure 2(a) shows the excitation energy spectrum obtained for the  $^{16}\text{O} + ^{16}\text{O}$  breakup for the data taken at the  $14^\circ/14^\circ$  arm angle setting. Despite the low statistics there is evidence for several peaks in the 32–38 MeV excitation energy range. The overall profile of the spectrum is modified by the variation of the coincidence detection efficiency with excitation energy. The efficiency profile has been determined by a Monte Carlo simulation in which an exponentially decreasing cross section is assumed for the initial scattering [17]. An isotropic distribution is used for the subsequent breakup. The result of the simulation is shown by the solid curve through the solid squares, and indicates that the absence of events above 40 MeV in the excitation spectrum is

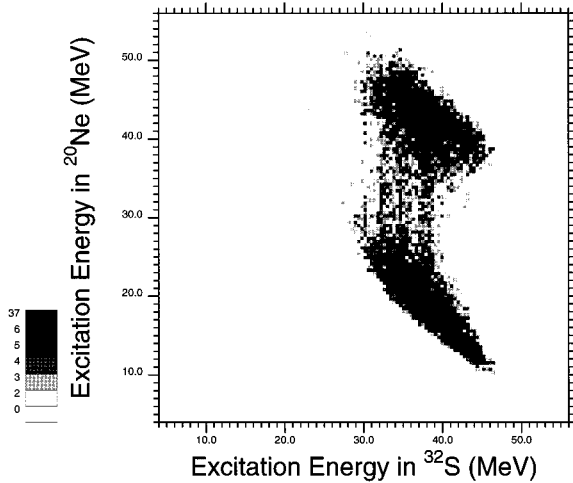


FIG. 3. Reconstructed excitation energy assuming  $^{16}\text{O} + ^{16}\text{O}$  breakup of  $^{32}\text{S}$  plotted against that calculated assuming  $^{16}\text{O} + ^4\text{He}$  breakup of  $^{20}\text{Ne}$ . Data for the two pairs of arm angles are combined.

a result of the falloff in efficiency with increasing energy. At excitation energies below 30 MeV the spectrum is suppressed by the proximity to the Coulomb barrier between the breakup fragments, which is indicated by the vertical arrow.

Figure 2(b) shows the excitation energy spectrum obtained from the data taken at the  $18^\circ/18^\circ$  arm angle setting, together with the corresponding efficiency profile. As in Fig. 2(a) several peaks may be seen within the overall profile of the spectrum. Two of the peaks (at 34.7 MeV and 35.6 MeV) seen in Fig. 2(b) can also be seen in Fig. 2(a), suggesting that they represent true states and are not simply an effect of the low statistics. The predicted experimental resolution in the reconstructed excitation energy spectrum, obtained from a Monte Carlo simulation of the reaction, is  $(300 \pm 30)$  keV. This Monte Carlo calculation was similar to that performed for the total energy spectrum.

One assumption made in the analysis of this data is that the detected  $^{16}\text{O}$  nuclei are fragments from the breakup of  $^{32}\text{S}$ . It would be possible, however, to produce the same exit channel particles from the  $^{12}\text{C}(^{24}\text{Mg}, ^{20}\text{Ne}^*)^{16}\text{O}$  reaction, followed by breakup of the excited  $^{20}\text{Ne}$  nucleus to  $^{16}\text{O} + ^4\text{He}$ . If such a process were to occur, then the reconstructed excitation energy of the  $^{20}\text{Ne}$  nucleus, determined by calculating the relative energy between one of the two  $^{16}\text{O}$  nuclei and the  $^4\text{He}$  particle, may show structure corresponding to breakup from specific excited states in  $^{20}\text{Ne}$ . Figure 3 shows a two-dimensional plot of the excitation energy as calculated assuming  $^{16}\text{O} + ^{16}\text{O}$  breakup of  $^{32}\text{S}$  against that calculated assuming the  $^{16}\text{O} + ^4\text{He}$  breakup of  $^{20}\text{Ne}$ , for the combined data taken at both  $14^\circ/14^\circ$  and  $18^\circ/18^\circ$  arm angle settings. It is possible to see vertical loci corresponding to the states seen in Figs. 2(a) and 2(b) in this plot. Although there is little evidence for horizontal loci, there is some evidence at the top of the plot for diagonal correlations. Such loci could arise if fragments from the  $^{12}\text{C}(^{24}\text{Mg}, ^{20}\text{Ne}^*)^{16}\text{O}$  reaction were indeed being detected, but with the reconstruction being performed between the  $\alpha$  particle and the wrong  $^{16}\text{O}$  nucleus.

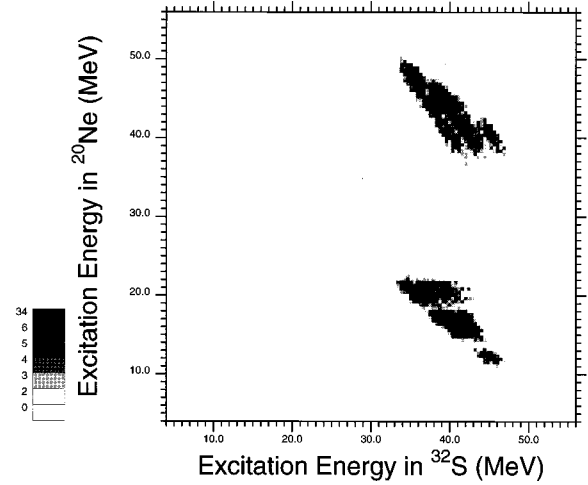


FIG. 4. A Monte Carlo simulation of the reaction  $^{12}\text{C}(^{24}\text{Mg}, ^{20}\text{Ne}^*)^{16}\text{O}, ^{20}\text{Ne}^* \rightarrow ^{16}\text{O} + ^4\text{He}$  for excitation energies in  $^{20}\text{Ne}$  corresponding to states seen by Rae *et al.* [18] in the  $^{12}\text{C}(^{16}\text{O}, ^{20}\text{Ne}^*)^8\text{Be}$  reaction.

To investigate further the contribution from the  $^{16}\text{O} + ^4\text{He}$  breakup of excited states in  $^{20}\text{Ne}$  we have performed extensive Monte Carlo simulations of the  $^{12}\text{C}(^{24}\text{Mg}, ^{20}\text{Ne}^*)^{16}\text{O}, ^{20}\text{Ne}^* \rightarrow ^{16}\text{O} + ^4\text{He}$  reaction, in which the exact geometries and electronic thresholds of the experiment were used. The states in  $^{20}\text{Ne}$  between 9 and 21 MeV of excitation which were observed in  $^{16}\text{O} + ^4\text{He}$  breakup following the  $^{12}\text{C}(^{16}\text{O}, ^{20}\text{Ne}^*)^8\text{Be}$  reaction [18] were simulated in turn. The pseudodata from this simulation was then analyzed in the same way as the real data. Figure 4 shows a two-dimensional plot of  $E(^{16}\text{O}-^{16}\text{O})$  versus  $E(^{16}\text{O}-^4\text{He})$  (similar to the plot in Fig. 3) from this analysis. The upper set of diagonal loci represents events where the incorrect  $^{16}\text{O}$ , the recoiling-target-like nucleus, has been associated with the  $^4\text{He}$ . The lower horizontal loci correspond to the correct  $^{16}\text{O}$ , the breakup fragment, being associated with the  $^4\text{He}$ . Between the two lobes corresponding to the  $^{12}\text{C}(^{24}\text{Mg}, ^{20}\text{Ne}^*)^{16}\text{O}$  reaction in Fig. 4 is a clear region. Any data in this region in Fig. 3 should therefore correspond to the  $^{12}\text{C}(^{24}\text{Mg}, ^{16}\text{O})^{16}\text{O}^4\text{He}$  reaction. Figure 5 shows the results from a similar Monte Carlo simulation of the  $^{12}\text{C}(^{24}\text{Mg}, ^{16}\text{O})^{16}\text{O}^4\text{He}$  reaction for states at energies corresponding to those seen in Figs. 2(a) and 2(b). As expected this shows vertical loci in the two-dimensional plot. The Monte Carlo simulations provide a very consistent description of the results shown in Fig. 3. The simulations suggest that by placing a software window about the central region of the data in Fig. 3, the genuine  $^{16}\text{O} + ^{16}\text{O}$  states can be separated from the background of  $^{16}\text{O} + ^4\text{He}$  states. The excitation energy spectrum produced by such a gating is shown in Fig. 6, where there is much clearer evidence for discrete states at energies of approximately 33, 35, and 38 MeV.

Integrating the data appearing in Figs. 2(a) and 2(b) allowed upper limits for the integrated double differential cross section for the  $^{16}\text{O} + ^{16}\text{O}$  breakup of  $^{32}\text{S}$  to be obtained. The resultant values are  $d^2\sigma/d\Omega_1 d\Omega_2 = (0.19 \pm 0.03)$  mb  $\text{sr}^{-2}$  for the  $14^\circ/14^\circ$  arm angle setting and  $d^2\sigma/d\Omega_1 d\Omega_2 =$

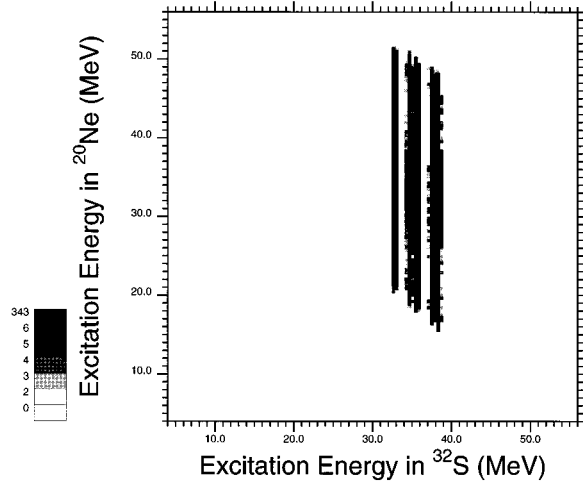


FIG. 5. A Monte Carlo simulation of the reaction  $^{12}\text{C}(^{24}\text{Mg}, ^{16}\text{O})^4\text{He}$  for excitation energies in  $^{32}\text{S}$  corresponding to the states seen in Figs. 2(a) and 2(b).

$(0.21 \pm 0.03) \text{ mb sr}^{-2}$  for the data obtained at  $18^\circ/18^\circ$ . It is noted that these cross sections include background statistics from the  $^{12}\text{C}(^{24}\text{Mg}, ^{20}\text{Ne}^*)^{16}\text{O}$  reaction as seen from Figs. 4 and 5, where the loci for the  $^{12}\text{C}(^{24}\text{Mg}, ^{16}\text{O})^4\text{He}$  reaction states are seen to extend into the region of data associated with the  $^{16}\text{O} + ^4\text{He}$  breakup of  $^{20}\text{Ne}$ . Placing a software window about the central region of the data in Fig. 3 to obtain the filtered excitation energy spectrum shown in Fig. 6 therefore caused some of the data from the  $^{16}\text{O} + ^{16}\text{O}$  breakup of  $^{32}\text{S}$  to be rejected. By integrating the  $18^\circ/18^\circ$  arm angle setting events seen in Fig. 6 a lower limit on the integrated double differential cross section was obtained,  $d^2\sigma/d\Omega_1 d\Omega_2 = (0.062 \pm 0.002) \text{ mb sr}^{-2}$ .

In order to determine the spins of the observed states, two-dimensional angular correlation plots were made by windowing on each of the peaks seen in Fig. 6. The angles used for the correlations are  $\theta^*$ , the center of mass scattering angle of the excited  $^{32}\text{S}$  nucleus, and  $\psi$ , the angle between

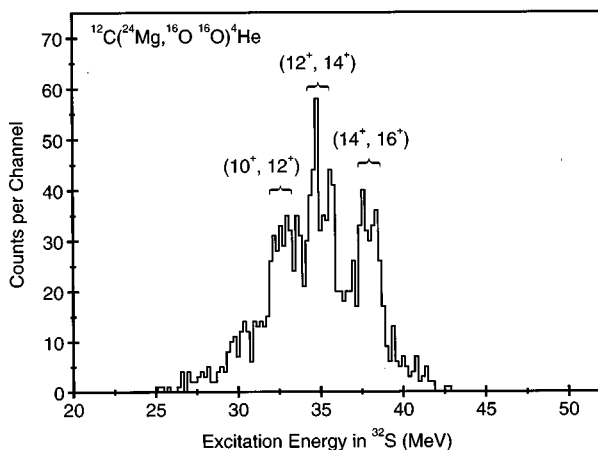


FIG. 6. Excitation energy spectrum for  $^{16}\text{O} + ^{16}\text{O}$  breakup of  $^{32}\text{S}$  for events gated on a selected region of Fig. 3. Data for the two pairs of arm angles are combined.

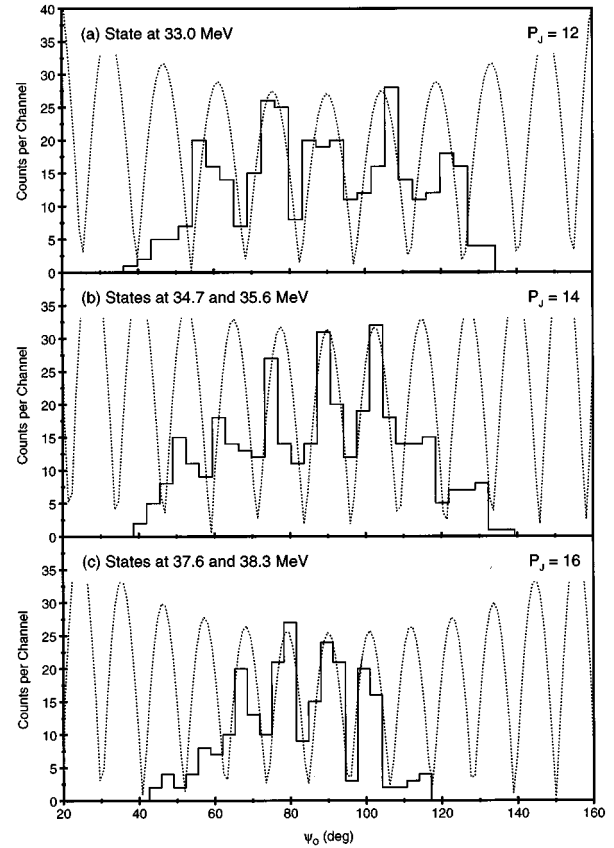


FIG. 7. Experimental angular correlation projections onto the  $\theta^*=0$  ( $\psi$ ) axis (solid histograms) for (a) the state at 33.0 MeV overlaid with a Legendre polynomial of order 12 (dotted line), (b) the states at 34.7 and 35.6 MeV overlaid with a Legendre polynomial of order 14, and (c) the states at 37.6 and 38.3 MeV overlaid with a Legendre polynomial of order 16.

the  $^{16}\text{O}$ - $^{16}\text{O}$  breakup vector and the beam axis. These angles have been defined for example by Marsh and Rae [19]. The angular correlations reveal ridges in the  $\theta^*/\psi$  space [19,20] which have a characteristic gradient given by  $J/l_{\text{GF}}$ , where  $J$  represents the spin of the state and  $l_{\text{GF}}$  the grazing angular momentum of the final state outgoing resonant particle [21]. Projecting these ridges onto the ( $\theta^*=0$ )  $\psi$  axis at an angle which is parallel to the gradient of the ridges allows a Legendre polynomial to be overlaid on the correlations, of the form  $|P_J[\cos(\psi)]|^2$  [6]. The Legendre polynomials most closely describing the correlations with the peaks near 33, 35, and 38 MeV are shown in Figs. 7 and 8.

Figure 7(a) shows a Legendre polynomial of order  $J = 12$  overlaid onto the projection of the  $\theta^*/\psi$  plot for the state centered at 33 MeV. The angle of projection of the  $\theta^*/\psi$  plot used to produce the projection shown in Fig. 7(a) yields the gradient  $J/l_{\text{GF}}$ . Assuming alignment of the angular momentum in the reaction then  $l_{\text{GI}} = J + l_{\text{GF}}$  [22], and from this the grazing angular momentum of the initial incoming particle,  $l_{\text{GI}}$ , is calculated to be  $(26.6 \pm 1.6)\hbar$ . Figure 7(b) shows a Legendre polynomial of order  $J = 14$  overlaid onto the projection for the two states centered at 35 MeV, for which the projection angle yields  $l_{\text{GI}} = (29.2 \pm 1.7)\hbar$ . The projection for the states centered at 38 MeV is shown in Fig. 7(c). In this figure a Legendre polynomial of order  $J = 16$  is overlaid

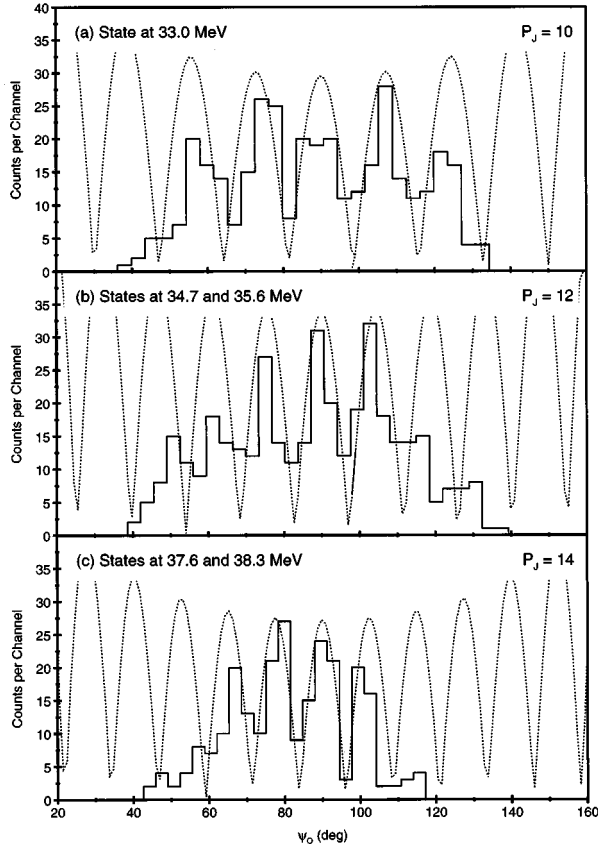


FIG. 8. Experimental angular correlation projections onto the  $\theta^* = 0$  ( $\psi$ ) axis (solid histograms) for (a) the state at 33.0 MeV overlaid with a Legendre polynomial of order 10 (dotted line), (b) the states at 34.7 and 35.6 MeV overlaid with a Legendre polynomial of order 12, and (c) the states at 37.6 and 38.3 MeV overlaid with a Legendre polynomial of order 14.

onto the projection, the projection angle yielding  $l_{\text{GI}} = (29.9 \pm 1.8)\hbar$ . Alternative polynomials may be overlaid on these projections, yielding values of  $P_J = 10$  for  $E_x \sim 33$  MeV, for which  $l_{\text{GI}}$  is calculated to be  $(22.2 \pm 1.4)\hbar$ , shown in Fig. 8(a). For the states centered at  $E_x \sim 35$  MeV, a polynomial of  $P_J = 12$  may also be overlaid on the projection, yielding  $l_{\text{GI}} = (25.0 \pm 1.4)\hbar$ . This is shown in Fig. 8(b). In Fig. 8(c) the projection for the states centered at  $E_x \sim 38$  MeV is shown overlaid with a polynomial of  $P_J = 14$ , for

which  $l_{\text{GI}} = (26.2 \pm 1.6)\hbar$ . The excitation energies of the states seen in Fig. 6 are listed in Table I, as are the proposed spin assignments and deduced grazing angular momenta of the initial incoming particle,  $l_{\text{GI}}$ .

In order to distinguish between these alternative values of  $l_{\text{GI}}$ , a series of distorted-wave Born approximation (DWBA) calculations was made for the  $^{12}\text{C}(^{24}\text{Mg}, ^{32}\text{S}^*)^4\text{He}$  reaction. In the calculations the  $^{32}\text{S}$  was assumed to be excited to states of energy (spin) of 33 MeV ( $10^+$  and  $12^+$ ), 35 MeV ( $12^+$  and  $14^+$ ), and 38 MeV ( $14^+$  and  $16^+$ ). The optical parameters of Daneshavar *et al.* [23] were used to generate the distorted waves, and the bound states of the transferred  $^8\text{Be}$  clusters were calculated in a conventional Woods-Saxon well with parameters  $R = 1.25(A^{1/3} + 8^{1/3})$  fm and  $a = 0.65$  fm, using  $2N + l = 20$  for the  $s$ - $d$  shell and  $2N + l = 8$  for the  $p$  shell. Figure 9 shows the partial cross sections versus partial wave number for these calculations. It is seen in Fig. 9(a) that for a state at  $E_x = 33$  MeV and spin  $J = 10^+$  the peak contribution is near a partial wave number  $l_{\text{GI}} = 24\hbar$ , while for the  $J = 12^+$  state the peak contribution lies nearer  $l_{\text{GI}} = 26\hbar$ . For a state at an excitation energy of 35 MeV and spin  $J = 12^+$  the peak contribution lies near  $l_{\text{GI}} = 25\hbar$  and, for  $J = 14^+$ ,  $l_{\text{GI}} = 27\hbar$ , Fig. 9(b). Figure 9(c) shows that for a  $J = 14^+$  state at  $E_x = 38$  MeV the peak contribution is  $\sim l_{\text{GI}} = 26\hbar$ , and for  $J = 16^+$  the peak contribution lies close to  $l_{\text{GI}} = 28\hbar$ . The calculated values of the initial grazing angular moment  $l_{\text{GI}}$  are listed in Table I for comparison with the experimental values obtained in the present work. It is seen that the calculations lend support to the values of  $l_{\text{GI}}$  extracted from the slopes of the angular correlations, but are unable to distinguish between the assignments of ( $10^+$  or  $12^+$ ), ( $12^+$  or  $14^+$ ), and ( $14^+$  or  $16^+$ ).

Figure 10 shows the known  $^{16}\text{O} + ^{16}\text{O}$  scattering resonances on a plot of energy against spin (taken from Cindro [7]). The locus of the resonances is consistent with a rotational sequence. The solid horizontal lines show the location of the states observed in the present breakup measurement. These appear to lie on the same trajectory as the scattering resonances, suggesting that the same underlying structure is being observed in the two measurements.

By considering these states in  $^{32}\text{S}$  as members of a deformed rotational band with excitation energies  $E_x = E_0 + (\hbar^2/2\mathcal{I})J(J+1)$  we can obtain the gradient of  $E_x$  versus  $J$  as  $\hbar^2/2\mathcal{I} = 49$  keV (for spins of  $10^+$ ,  $12^+$ , and  $14^+$ ) or 42 keV (for spins of  $12^+$ ,  $14^+$ , and  $16^+$ ). These values agree

TABLE I. List of excitation energies, proposed spins, and deduced grazing angular momenta in the entrance channel ( $l_{\text{GI}}$ ) for the states seen in Fig. 6. The calculated values of  $l_{\text{GI}}$  are also listed. The states at 34.69 and 35.64 MeV and also those at 37.55 and 38.32 MeV were paired together in order to make the spin assignments as listed.

$E_x$ (MeV)	Proposed spin ( $\hbar$ )	Deduced $l_{\text{GI}}$ ( $\hbar$ )	Calculated $l_{\text{GI}}$ ( $\hbar$ )
$33.03 \pm 0.12$	10	$22.2 \pm 1.4$	$\sim 24$
	12	$26.6 \pm 1.6$	$\sim 26$
$34.69 \pm 0.08$ and $35.64 \pm 0.06$	12	$25.0 \pm 1.4$	$\sim 25$
	14	$29.2 \pm 1.7$	$\sim 27$
$37.55 \pm 0.11$ and $38.32 \pm 0.12$	14	$26.2 \pm 1.6$	$\sim 26$
	16	$29.9 \pm 1.8$	$\sim 28$

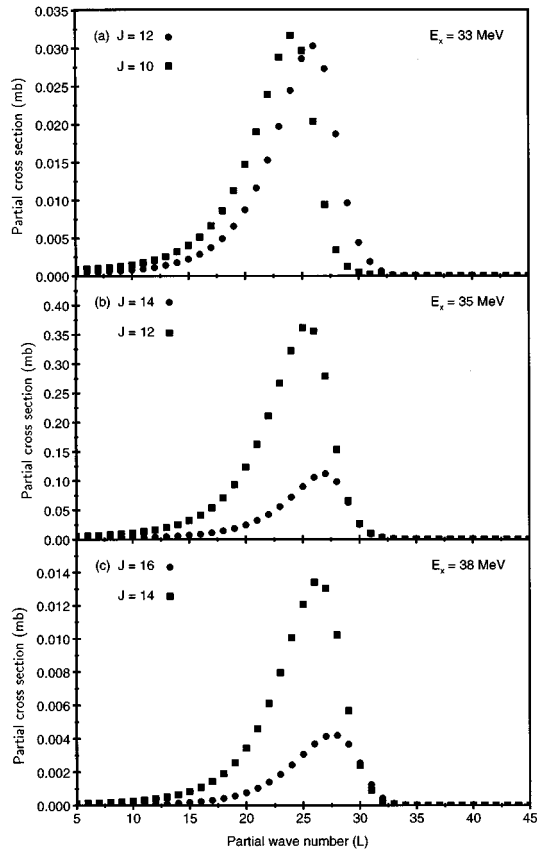


FIG. 9. Partial cross section versus partial wave number obtained from DWBA calculations of the reaction  $^{12}\text{C}(^{24}\text{Mg}, ^{32}\text{S}^*) ^4\text{He}$  for excitations of (a) a  $J=10^+$  state at 33 MeV (solid squares) and a  $J=12^+$  state at 33 MeV (solid circles), (b) a  $J=12^+$  state at 35 MeV (solid squares) and a  $J=14^+$  state at 35 MeV (solid circles), and (c) a  $J=14^+$  state at 38 MeV (solid squares) and a  $J=16^+$  state at 38 MeV (solid circles).

well with the observed  $^{16}\text{O} + ^{16}\text{O}$  scattering resonance data rotational trajectory, and are also in agreement with the corresponding parameter calculated by Cindro for two touching  $^{16}\text{O}$  nuclei in a dimolecular configuration, 43.3 keV [7]. Such a gradient is indicated in Fig. 10 by the dashed diagonal line, and it can be seen that the rotational spacing of the calculation agrees well with the breakup data and the scattering resonances (it is noted that vertical position of the line is arbitrary, as the band head energy  $E_0$  is not determined in the calculations of Cindro).

#### IV. SUMMARY

A study of the  $^{12}\text{C}(^{24}\text{Mg}, ^{16}\text{O} \ ^{16}\text{O}) ^4\text{He}$  reaction has revealed the  $^{16}\text{O} + ^{16}\text{O}$  breakup of  $^{32}\text{S}$ . A number of states has been observed in the reconstructed excitation energy spectrum of the resonant  $^{32}\text{S}$  nucleus in the 32–38 MeV excita-

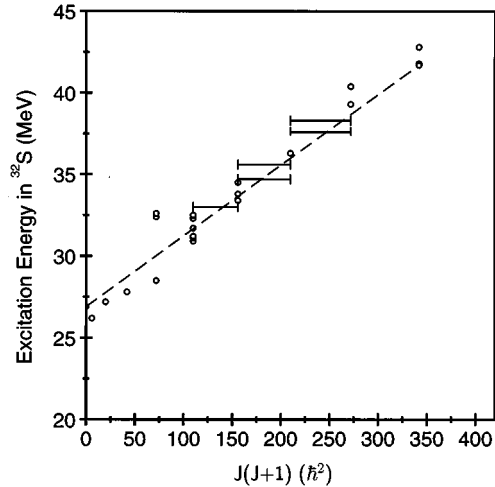


FIG. 10. Energy-spin systematics for the  $^{16}\text{O} + ^{16}\text{O}$  scattering resonances listed by Cindro [7], represented by the open circles. The solid horizontal lines represent the states observed in the present breakup measurement. The dashed diagonal line represents the rotational parameter calculated by Cindro for two touching  $^{16}\text{O}$  nuclei in a dimolecular configuration.

tion energy range. Projections of angular correlations for states near 33, 35, and 38 MeV, supported by DWBA calculations, suggest spins in the range  $10^+ - 16^+$ , placing the states on the locus of resonances observed in  $^{16}\text{O} + ^{16}\text{O}$  scattering, and yielding a rotational parameter of  $\hbar^2/2\mathcal{I}$  in the range 42–49 keV. These discrete states are similar in nature to those seen in the  $^{12}\text{C} + ^{12}\text{C}$  breakup of  $^{24}\text{Mg}$  and may be indicative of similar underlying nuclear structure effects. Both alpha cluster model and Nilsson-Strutinsky calculations predict the existence of highly deformed shape isomeric states in  $^{32}\text{S}$  in this excitation region. However, in order to make a more conclusive association between the observed states and these deformed configurations (and the resonances observed in  $^{16}\text{O} + ^{16}\text{O}$  scattering studies) it is clear that a higher resolution measurement is needed not only for a detailed study of the excitation spectrum but for the confirmation of the spins of the states obtained in this measurement.

#### ACKNOWLEDGMENTS

The authors would like to acknowledge the financial support of the Engineering and Physical Sciences Research Council (EPSRC). N.C., A.M., M.J.L., J.S.P., S.M.S., S.P.G.C., S.P.F., and P.M.S. would like to thank EPSRC for individual financial support. The cooperation and assistance of the staff of the 14UD accelerator facility at the Australian National University (ANU) are gratefully appreciated. This work was carried out under a formal collaboration agreement between EPSRC and ANU.

[1] A.M. Sandorfi, J.R. Calarco, R.E. Rand, and H.A. Schwettman, Phys. Rev. Lett. **45**, 1615 (1980).  
 [2] C.A. Davies, G.A. Moss, G. Roy, J. Uegaki, R. Abegg, L.G.

Greeniaus, D.A. Hutcheon, and C.A. Miller, Phys. Rev. C **35**, 336 (1987).

[3] S. Lawitzki, D. Pade, B. Gonsior, C.D. Uhlhorn, S. Branden-

- burg, M.N. Harakeh, and H.W. Wilschut, *Phys. Lett. B* **174**, 246 (1986).
- [4] J. Wilczynski, K. Siwek-Wilczynska, Y. Chan, S.B. Gazes, and R.G. Stokstad, *Phys. Lett. B* **181**, 229 (1986).
- [5] B.R. Fulton, S.J. Bennett, C.A. Ogilvie, J.S. Lilley, D.W. Banes, W.D.M. Rae, S.C. Allcock, R.R. Betts, and A.E. Smith, *Phys. Lett. B* **181**, 233 (1986).
- [6] B.R. Fulton, S.J. Bennett, M. Freer, J.T. Murgatroyd, G.J. Gyapong, N.S. Jarvis, C.D. Jones, D.L. Watson, J.D. Brown, W.D.M. Rae, A.E. Smith, and J.S. Lilley, *Phys. Lett. B* **267**, 325 (1991).
- [7] N. Cindro, *Ann. Phys. (Paris)* **13**, 289 (1988).
- [8] N. Curtis, N.M. Clarke, B.R. Fulton, S.J. Hall, M.J. Leddy, A.St.J. Murphy, J.S. Pople, R.P. Ward, W.N. Catford, G.J. Gyapong, S.M. Singer, S.P.G. Chappell, S.P. Fox, C.D. Jones, D.L. Watson, W.D.M. Rae, and P.M. Simmons, *Phys. Rev. C* **51**, 1554 (1995).
- [9] S.J. Bennett, M. Freer, B.R. Fulton, J.T. Murgatroyd, P.J. Woods, S.C. Allcock, W.D.M. Rae, A.E. Smith, J.S. Lilley, and R.R. Betts, *Nucl. Phys.* **A534**, 445 (1991).
- [10] G. Leander and S.E. Larsson, *Nucl. Phys.* **A239**, 93 (1975).
- [11] M. Flocard, P.H. Heenen, S.J. Krieger, and M.S. Weiss, *Prog. Theor. Phys.* **72**, 100 (1984).
- [12] J. Zhang, W.D.M. Rae, and A.C. Merchant, *Nucl. Phys.* **A575**, 61 (1994).
- [13] M. Harvey, in *Many nucleon correlations in light nuclei*, Proceedings of the Second International Conference on Clustering Phenomena in Nuclei, edited by D.A. Goldberg, USDERA Report No. ORO-4856-26, 1975 (unpublished), p. 549.
- [14] U. Mosel, *Structure and formation of molecules*, Lecture Notes in Physics Vol. 156 (Springer-Verlag, Berlin, 1981), p. 358.
- [15] M. Freer, R.R. Betts, and A.H. Wuosmaa, *Nucl. Phys.* **A587**, 36 (1995).
- [16] N. Curtis, A.St.J. Murphy, M.J. Leddy, J.S. Pople, N.M. Clarke, M. Freer, B.R. Fulton, S.J. Hall, G. Tungate, R.P. Ward, S.M. Singer, W.N. Catford, G.J. Gyapong, R.A. Cunningham, J.S. Lilley, S.P.G. Chappell, S.P. Fox, C.D. Jones, D.L. Watson, P.M. Simmons, R.A. Hunt, A.C. Merchant, A.E. Smith, W.D.M. Rae, and J. Zhang, *Nucl. Instrum. Methods Phys. Res. Sect. A* **351**, 359 (1994).
- [17] R.R. Betts, S.B. Di Cenzo, M.H. Mortensen, and R.L. White, *Phys. Rev. Lett.* **39**, 1183 (1977).
- [18] W.D.M. Rae, A.J. Cole, B.G. Harvey, and R.G. Stokstad, *Phys. Rev. C* **30**, 158 (1984).
- [19] S. Marsh and W.D.M. Rae, *Phys. Lett.* **153B**, 21 (1985).
- [20] W.D.M. Rae and R.K. Bhowmik, *Nucl. Phys.* **A420**, 320 (1984).
- [21] E.F. Da Silveira, in *Effects of reaction mechanisms on particle-particle angular correlation*, Proceedings of the 14th Winter Meeting on Nuclear Physics, Bormio, 1976 (unpublished), p. 293.
- [22] M. Freer, N.M. Clarke, N. Curtis, B.R. Fulton, S.J. Hall, M.J. Leddy, J.S. Pople, G. Tungate, R.P. Ward, P.M. Simmons, W.D.M. Rae, S.P.G. Chappell, S.P. Fox, C.D. Jones, D.L. Watson, G.J. Gyapong, S.M. Singer, W.N. Catford, and P.H. Regan, *Phys. Rev. C* **51**, 1682 (1995).
- [23] K. Daneshavar, D.G. Kovar, S.J. Krieger, and K.T.R. Davies, *Phys. Rev. C* **25**, 1342 (1982).